

Local Tolerability and Performance Evaluation in Domestic Pigs of a Fractional Radiofrequency Device for Dermatologic Treatment

Toxicologic Pathology

1-8

© The Author(s) 2020

Article reuse guidelines:

sagepub.com/journals-permissions

DOI: 10.1177/0192623320922958

journals.sagepub.com/home/tpx



Yuval Ramot¹ , Guy Klaiman², Michal Steiner², Yossi Lavie², Inna Belenky³, and Abraham Nyska⁴

Abstract

Information on the safety of energy-based dermatological surgical devices in domestic pigs, and fractional radiofrequency (RF) devices in particular, is very limited. The aim of this study was to evaluate in a GLP-compliant study in domestic pigs the local reaction and performance of a novel fractional RF device. Five female domestic pigs were subjected to fractional RF pulses, using different energy and pulse durations and depth of penetration of the pulses. The animals were evaluated clinically and histologically at different time points (days 0, 1, 3, 7, and 14) postenergy exposure. There were no microscopic or macroscopic local adverse effects in any tested power settings, and there was time-related progressive healing, reaching complete macroscopic and microscopic healing by 7 days postapplication. As expected, there was power-related progressive increase in the incidence of ablation (destruction of skin tissue by vaporization) and coagulative necrosis of the dermis from low to high power setting. This comprehensive study, using multiple power settings (both ablative and coagulative) and several time points, will be of benefit for future studies evaluating new fractional RF devices.

Keywords

animal studies, radiofrequency, lasers, domestic pig, medical devices

Introduction

Energy-based devices have gained much popularity in the last years for the treatment of a wide array of medical conditions, such as skin aging, pigmentation, and traumatic and acne scars.^{1,2} Ablative methods are usually used for skin resurfacing, and work by removing the epidermis and the upper component of the dermis. This results in neocollagenesis and remodeling.^{3,4} The ablative effects are achieved by vaporization, when the temperature of the skin reaches 100°C.⁵ Non-ablative devices conserve the epidermis from ablation and result in thermal injury only in the dermis.⁴ These devices deliver radiofrequency (RF)-based energy (alternating electric current), resulting in movement of charged particles, that ultimately leads to the production of thermal energy.^{6,7} When the skin temperature reaches 50°C, there is coagulation and necrosis of the dermis, leading to the formation of new cells.⁸

In 2004, a fractional laser was introduced, enabling the production of microscopic treatment zones and preserving the healthy tissue between these treatment columns.⁹ This technology has since been applied to both the ablative and non-ablative methods and allowed reduced time to recovery and less complications, such as cutaneous and vascular necrosis,

scarring, erosions, burns, purpura, and pigmentary changes, compared to full (non-fractional) ablative lasers.^{10,11} Shortly, following the fractional lasers, fractional RF technologies were introduced to the market. The first generation of fractional RF devices could not produce deep coagulative necrosis solely and resulted also in ablation of the epidermal layer, while ablation of the epidermis also led to coagulation/necrosis of the upper dermis.^{8,12,13} A newer second-generation RF device is able to generate separate biological effects, that is, coagulation, ablation, or both, thereby providing better flexibility and adjustability for the user.^{8,12,13}

¹ Hadassah Medical Center, The Faculty of Medicine, Hebrew University of Jerusalem, Jerusalem, Israel

² Envigo CRS (Israel), Ness Ziona, Israel

³ Viora Ltd, New York, NY, USA

⁴ Toxicologic Pathology, Tel Aviv University, Timrat, Israel

Corresponding Author:

Abraham Nyska, Toxicologic Pathology, Tel Aviv University, Haharuv 18, P.O. Box 184, Timrat 36576, Israel.

Email: anyska@bezeqint.net

Table 1. Activation Site Parameters.

Group	No. of Activation Sites	Program	Settings		Additional Functions Cooling, Vacuum, Smart Heat
			Energy (J)	Pulse Duration (ms)	
1	5		Untreated control		
2	25	Shallow	3	100	On
3	25		5	60	On
4	25		8	10	On
5	25	Medium	3	100	On
6	25		5	60	On
7	25		8	10	On
8	25	Deep	3	100	On
9	25		5	60	On
10	25		8	10	On
11	25	Shallow	10	10	On
12	25	Shallow	10	10	Off

Abbreviations: J, joules; ms, milliseconds.

While fractional RF devices are commonly used, their application can sometimes be accompanied by complications. Indeed, all energy-based devices should be submitted for a premarket evaluation by the US Food and Drug Administration (FDA).¹⁴ In addition, it is necessary to evaluate the performance and safety of all medical devices, including fractional RF devices, in well-established and reliable preclinical GLP-compliant animal studies. Nevertheless, although fractional RF devices are abundantly used, information on preclinical studies with these devices is very sparse in the medical literature.^{15–17}

Here, we tested in a GLP-compliant study in domestic pigs the local reaction and performance of a novel fractional RF device (Viora Ltd., New York, New York), which uses the proprietary SVC technology, a combination of Switching, Vacuum and Cooling mechanisms.^{8,13} The Switching mechanism allows control of the depth of RF penetration to the skin (shallow, medium, or deep penetration), the Vacuum mechanism provides better coupling of the electrodes to the skin thereby decreasing pain levels, and the Cooling mechanism protects the superficial layers of the skin and decreases pain and side effects.

Materials and Methods

Animal Husbandry and Maintenance

Five female domestic swine (*Sus scrofa domestica*), with a weight range of 77 to 82.8 kg, were obtained from the institute of animal research—Kibbutz Lahav, Israel. Animals were requested to have no-to-minimal pigmentation at the abdomen. The animals were acclimatized to laboratory conditions for 9 days prior to study initiation. Temperatures were maintained at 16°C to 27°C with a relative humidity of about 30% to 70%, and a 12-h light/12-h dark cycle was set and maintained automatically. The studies were performed in Envigo CRS Israel Limited, Ness-Ziona, Israel, following an application form

review by the National Council for Animal Experimentation and after receiving its approval.

Experimental Design

Each animal was subjected to fractional RF pulses. Different settings, such as pulse energy (Joules) and pulse duration (10–100 ms), were adjusted between the different activation sites, influencing the total power of the treatment (Table 1): Low power settings (aimed for light coagulative response in humans)—3 Joules, 100 ms; Medium power settings (aimed for stronger coagulative response in humans)—5 Joules, 60 ms; High power settings (aimed for strongest ablative and coagulative response in humans)—8 Joules, 10 ms; Worst-case scenario (the highest possible power)—10 Joules, 10 ms; and Shallow program (providing maximum power on minimum skin surface). All 3 settings were tested at 3 programs of the device: Shallow, Medium, and Deep. All animals were applied 5 sets of the different 11 settings (9 operational and 2 worst-case scenarios) in predetermined positions at the animals' abdomen (Figure 1). All sites were evaluated macroscopically for local reaction at day 0, day 1, day 3, day 7, and at study termination 14 days postactivation. Skin biopsies were harvested from 1 example of each exposure condition from each animal on day 0, day 1, day 3, day 7, and at study termination 14 days postactivation. In order to minimize inadvertent bias, biopsy was performed from each animal on each collection day from a different set, enabling representation of all settings at different positions at the different time points (Supplemental Table 1). Harvested samples were processed histologically and evaluated for depth/width of the ablated tissue and coagulative necrosis.

Activation Procedure

On the day before the activation session, animals were subjected to food deprivation of at least 6 hours, while allowed free access to drinking water. Carprofen (Carprieve; Norbrook, Newry, Northern Ireland) at a dose level of 2 to 4 mg/kg as well as cefquinome (COBACTAN; InterVet, Boxmeer, Netherlands) at a dose level of 2 mg/kg were administered by subcutaneous injection (behind the ears, not at activation sites area). Animals were sedated by a combination of ketamine (8 mg/kg) and xylazine (1.6 mg/kg) administered intramuscularly (at the Gluteus muscles, away from the activation sites area). Anesthesia was further induced by inhalation of isoflurane 5% in 100% O₂ at a rate of 2 to 4 L/min via face mask. Throughout the session, isoflurane 1% to 3% was used to maintain anesthesia.

The hair was removed completely using electric clipper, while avoiding abrasion of the skin. The clipped area was scrubbed using 4% wt/vol chlorhexidine gluconate (SEPTAL SCRUB, TEVA Medical, Ashdod, Israel) and wiped with ethanol 70%. The tip of the device was placed in full contact with the skin at a 90-degree angle to the surface of the target region, at the center of the planned site, and activation was performed.

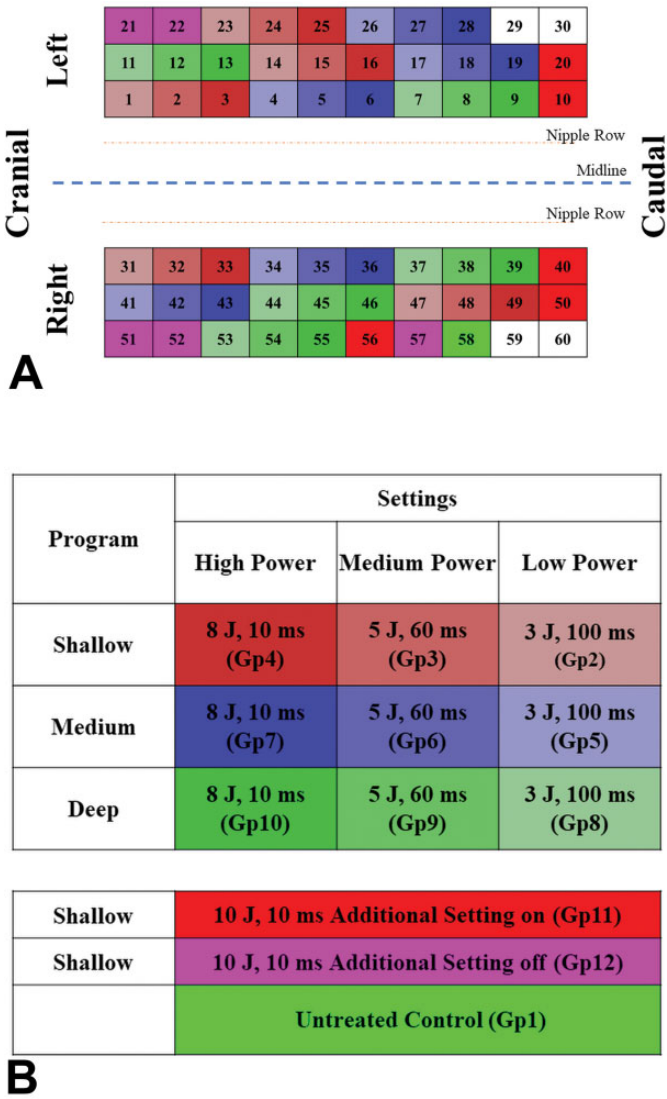


Figure 1. A, Schematic description of the activation sites on the animal's abdomen. B, Legend for the colors used in Figure 1.

Each activation site is in the size of 32.5 mm × 40 mm which is equivalent to the single use tip of the fractional RF device. The device was then moved to the next planned spot in the treatment area, and the procedure was repeated until all sites had been activated.

Following the activation, carprofen (Carprieve; Norbrook) for analgesia and cefquinome (COBACTAN; InterVet) for antibiotic prophylaxis were administered once daily for the duration of the study (14 days posttreatment) by the subcutaneous route at a dose of 2 to 4 and approximately 2 mg/kg, respectively.

Observations and Examinations

All animals were observed for mortality and general condition at least once daily. Macroscopic evaluation for erythema,

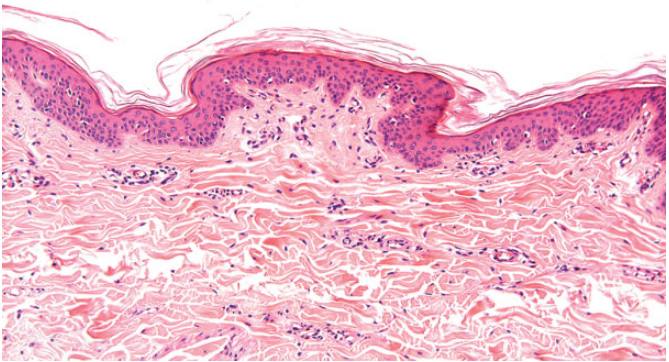


Figure 2. Histological section taken from a control untreated site, demonstrating the normal histopathological finding in the skin. H&E indicates hematoxylin and eosin.

edema, exudate, crust, and bleeding of all activation sites not yet biopsied was performed prior to each tissue harvesting on 0 (at least 30 minutes following application), 1, 3, 7, and 14 days postapplication. Degree of severity was scored on a scale of 0 to 4 (0—no erythema or edema, 1—very slight erythema or edema [barely perceptible], 2—well defined erythema or edema, 3—moderate to severe erythema or moderate edema [raised ~1 mm], and 4—severe erythema [beef redness] or severe edema [raised more than 1 mm]), except for exudate and bleeding, scored on a scale of 0 to 3 (0—none, 1—light, 2—moderate, 3—heavy).

In-life sampling of activation sites was performed at the end of the activation session (day 0) for each animal (at least 30 minutes following activation) and at 1, 3, 7, and 14 days post-treatment. Biopsies were harvested in anesthetized animals induced and maintained as described above. Each sample was excised from the center of the activation site with the full thickness of the skin (down to the underlying fat and subcutaneous tissue) using an 8-mm biopsy punch. Open wounds were sutured with appropriate suturing material (Assucryl 2-0, Assut Sutures, Lausanne, Switzerland), polydine solution was applied, and a stockinet was applied on the animal's body. Harvested samples were individually fixed in 10% neutral buffered formalin (approximately 4% formaldehyde solution).

Histology

All biopsies were bisected perpendicular to the skin surface and both halves were embedded in a paraffin block, to be sectioned perpendicular to the skin surface. Two, or in some cases 3, step histological sections (each approximately 5 microns thick and stained by hematoxylin and eosin [H&E]) were prepared from the surface of each half, at a depth of 100 microns and in some cases at an additional depth of 300 microns.

Histopathological evaluation included the following parameters: Size of ablated tissue—width and depth (morphometric

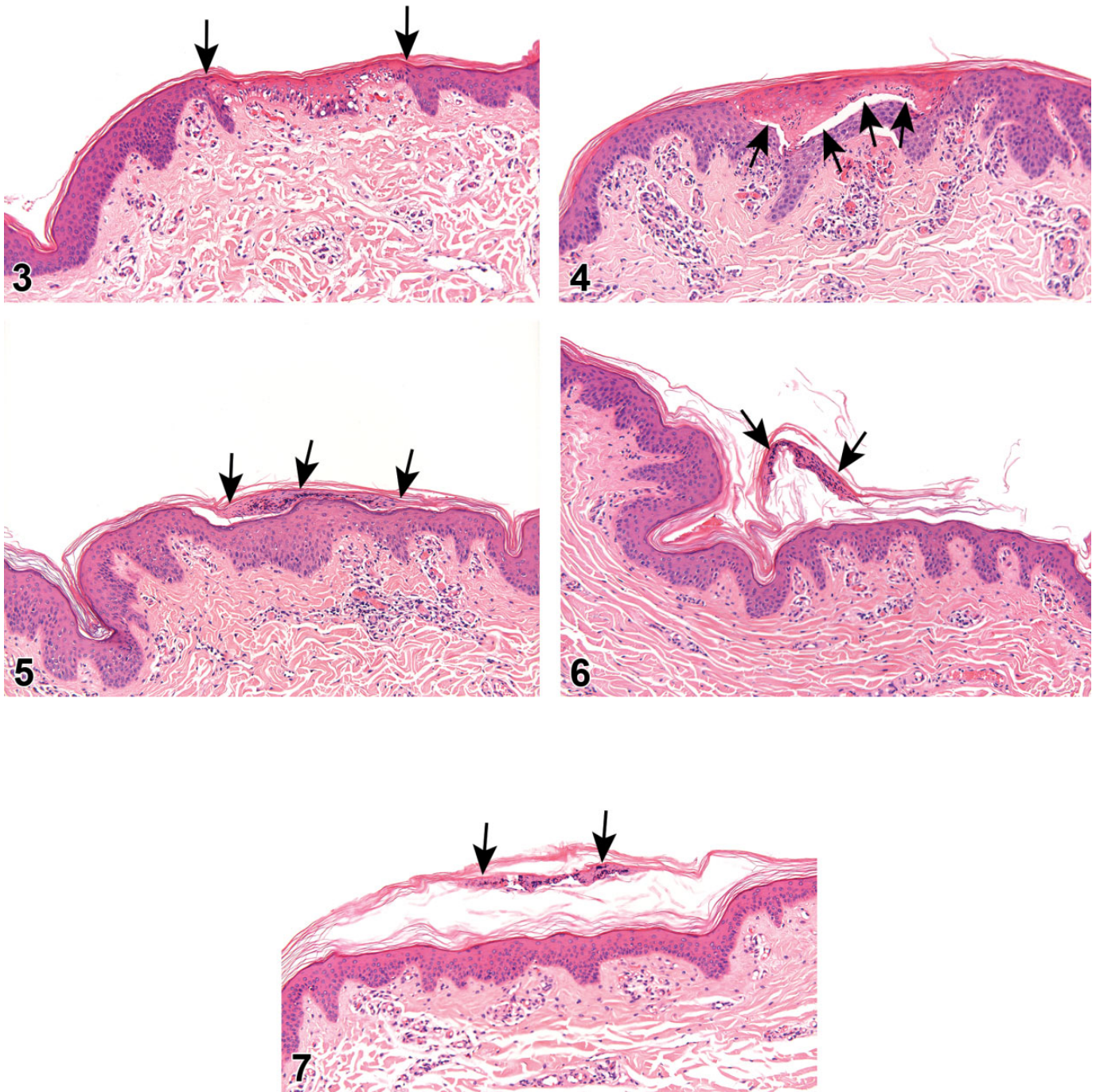


Figure 3–7. Figure 3. Histological section taken from group 3 (5 J of energy for the duration of 60 ms, Shallow program) at the end of the activation session (ie, day 0, at least 30 minutes following activation) showing a well circumscribed (ie, focal) epidermal coagulative necrosis (the outer margins of the coagulation necrosis are indicated by arrows). This focal epidermal change was not associated with any changes in the underlying deep dermis or subcutis. H&E indicates hematoxylin and eosin. **Figure 4.** Histological section taken from group 3 (5 J of energy for the duration of 60 ms) on day 1 post treatment. There is separation and detachment of the coagulated epidermis (arrows) with minimal inflammation located at the superficial epidermis, reflecting a clear trend for healing of the activation site. No changes were noted in the underlying deep dermis or subcutis. H&E indicates hematoxylin and eosin. **Figure 5.** Histological section taken from group 3 (5 J of energy for the duration of 60 ms) on day 3 posttreatment. There is a focal crust overlying the epidermis (arrows). The previously coagulated epidermis was completely replaced by newly formed epidermis, reflecting a clear trend for progressive healing of the activation site. No changes were noted in the deep dermis or subcutis. There is minimal perivascular mononuclear cell infiltration, which is a normal background finding in the Gottingen minipig. H&E indicates hematoxylin and eosin. **Figure 6.** Histological sections taken from group 3 (5 J of energy for the duration of 60 ms) on day 7 posttreatment.

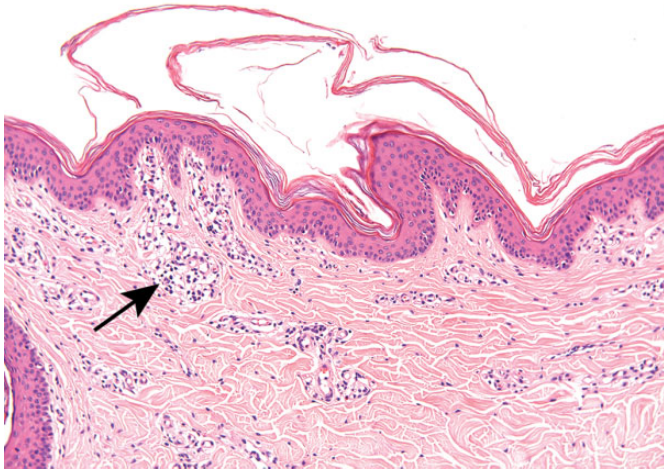


Figure 8. Histological section taken from a control untreated site, demonstrating the normal histopathological finding in the skin. There is focal mononuclear cell infiltration in the superficial dermis, which is considered to be a normal background change.

evaluation), size of coagulated tissue—width and depth (morphometric evaluation), presence of focal epidermal hyperplasia (ie, reflecting healing process) at the previously treated site (semiquantitative scoring), presence of focal dermal granulation tissue (ie, reflecting healing process) at the previously treated site (semiquantitative scoring), presence of focal epidermal crust at the previously treated site (semiquantitative scoring), and presence of focal inflammation at the previously treated site (semiquantitative scoring). Semiquantitative scoring was graded on a scale of 5 grades (0–4).¹⁸

Performance of the fractional RF device was based on macroscopic evaluation of the activation sites throughout the observation period and morphometric evaluation performed histologically and was based on the number of sites showing ablation and coagulation.

Statistical Analysis

Statistical analysis was performed using R (R-Studio version 0.99 as the interface) with a validated R-Script for statistical evaluation that performed the following: A normality test was performed considered Gaussian distribution (eg, Shapiro-Wilk normality test; $P < .01$). If the normality test passed for all groups an equal variance test was performed (eg, Bartlett test; $P < .01$). If the Bartlett test passed, 1-way analysis of variance with Dunnett posttest was performed. If the Bartlett test did not pass, Kruskal–Wallis test with Mann–Whitney U test was performed. If the normality test did not pass for all groups Kruskal–Wallis test with Mann–Whitney U test was performed.

Figure 3–7. (Continued). There is complete healing of the application site, with minimal exfoliating crust (arrows), without any inflammatory reaction at the adjacent or underlying tissue. H&E indicates hematoxylin and eosin. **Figure 7.** Histological sections taken from group 3 (5 J of energy for the duration of 60 ms) on day 14 posttreatment. There is complete healing of the application site, with minimal exfoliating crust (arrows), without any inflammatory reaction at the adjacent or underlying tissue. H&E indicates hematoxylin and eosin.

Results

Mortality, Clinical Observations, and Body Weight

No mortality or abnormal clinical signs were observed throughout the 14-day observation period. All animals made comparable body weight gain at the end of the observation period.

Macroscopic Evaluations

No exudate, crust, or bleeding was seen in any of the animals, except for 1 application site in 1 animal, where a small skin abrasion was noted 3 days postapplication and was attributed to self-inflicted rubbing of the animal against the surroundings and not to the treatment.

Up to 3 days postactivation, statistically significant higher group mean erythema score was limited to all groups treated with the high or worst-case scenario power settings (ie, power 8 J and 10 J, respectively, both for 10 ms; mean erythema score = 2) and to the group treated with medium power setting and deep program (mean erythema score = 1) compared to untreated control (Supplemental Table 2). Additionally, statistically significant higher group mean erythema score was noted at 7 days post activation for all groups treated with the high or worst-case scenario power settings (mean erythema score = 2) and at 14 days post activation for groups 4, 7, and 12 (mean erythema score = 1; Supplemental Table 2).

Edema was limited to activation sites treated with the high or worst-case scenario power settings (ie, power 8 J and 10 J, respectively, both for 10 ms) and statistically significant higher up to 1-day postactivation (mean erythema score = 1; Supplemental Table 3). At 3 days postactivation onward, sporadic incidences of edema were noted in the activation sites treated with high or worst-case scenario power settings, and no edema was noted from 7 days onward (Supplemental Table 3).

Histopathological Findings

Histopathological evaluation of the activation sites showed that all irradiation settings (penetration program, energy, and pulse duration) created a well circumscribed condensation of the epidermis (ie, coagulative necrosis), with short and complete healing process, without any complication (Figures 2–8).

On the day of activation (ie, day 0, about 30 minutes following activation), ablation (ie, loss of the epidermis and upper dermis) was noted in 93% of the high power-applied sites and in 80% and 100% of the worst-case scenario groups (Supplemental Table 4, Figure 9). Coagulative necrosis (of the deeper dermis) was observed in a power-dependent manner and seen in 100% of sites treated with the high or worst-case scenario power settings, 93% of cases treated with the medium power setting

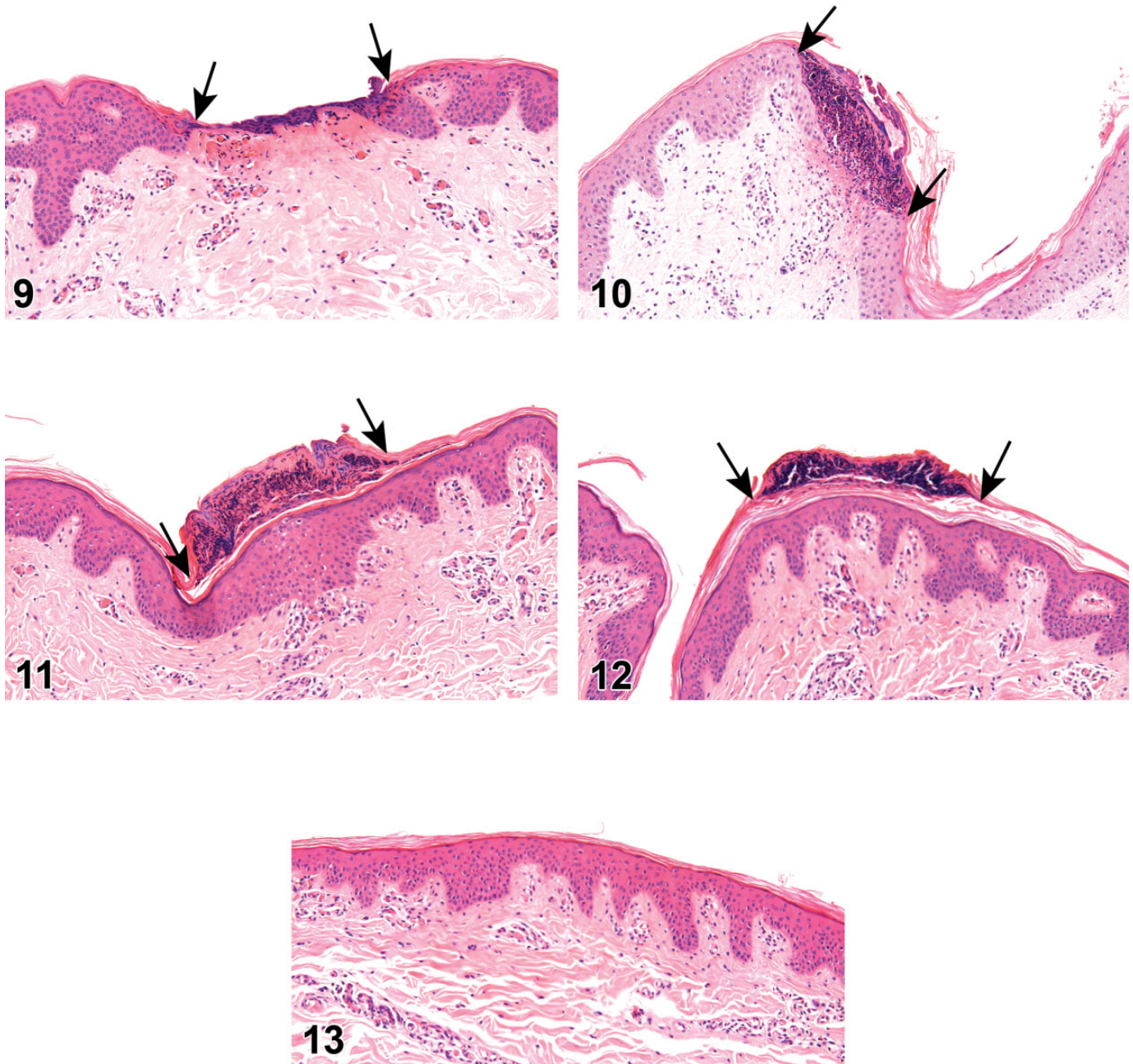


Figure 9–13. **Figure 9.** Histological section taken from group 10 (8 J of energy for the duration of 10 ms, deep program) at the end of the activation session (i.e. Day 0, at least 30 minutes following activation), showing a well-circumscribed (i.e., focal) epidermal ablation (the outer margins of the ablation are indicated by arrows). This focal epidermal change was associated with coagulative necrosis (i.e. hypereosinophilia) in the underlying superficial dermis, but not in the deep dermis or subcutis. H&E. **Figure 10.** Histological section taken from group 10 (8 J of energy for the duration of 10 ms) on day 1 posttreatment. The ablated epidermis (the outer margins of the ablation are indicated by arrows) is replaced by a crust, reflecting a clear trend for healing of the activation site. This focal epidermal change is associated with coagulative necrosis (ie, hypereosinophilia) in the underlying superficial dermis, but not in the deep dermis or subcutis. H&E indicates hematoxylin and eosin. **Figure 11.** Histological section taken from group 10 (8 J of energy for the duration of 10 ms) on day 3 posttreatment. There is a focal crust overlying the epidermis (arrows). The previously ablated epidermis was completely replaced by newly formed epidermis, reflecting a clear trend for progressive healing of the activation site. No changes were noted in the deep dermis or subcutis. H&E indicates hematoxylin and eosin. **Figure 12.** Histological section taken from group 10 (8 J of energy for the duration of 10 ms) on day 7 posttreatment. There is complete healing of the application site, with minimal exfoliating crust (arrows), without any inflammatory reaction at the adjacent or underlying tissue. H&E indicates hematoxylin and eosin. **Figure 13.** Histological section taken from group 10 (8 J of energy for the duration of 10 ms) on day 14 posttreatment. There is complete healing of the application site, without any inflammatory reaction at the adjacent tissue. H&E indicates hematoxylin and eosin.

and 80% of cases treated with the low power setting (Supplemental Table 5, Figure 3). In almost all the cases treated with the low or medium settings, coagulation was observed without ablation. On days 3, 7, and 14, there was complete healing of the application site, with minimal exfoliating crust, without any inflammatory reaction at the underlying tissue (Supplemental Tables 4 and 5; Figures 4–8, 10–13). In some of the sites, no crust was noted, and the superficial epidermis was normal in appearance. The focal epidermal and superficial dermal changes were not associated with any changes in the underlying deep dermis or subcutis. No epidermal hyperplasia or dermal granulation tissue was observed in any of the sections.

Discussion

The use of fractional RF devices is gaining increased popularity in recent years, and they are being utilized for a large number of indications, ranging from skin rejuvenation to treatment of scars. The indication being treated dictates the energy and duration parameters used in the device.⁸ For example, if skin resurfacing is indicated, the required effects is ablative in nature, and short duration with high RF energy will be used. If skin rejuvenation is required, the required effect is coagulative necrosis, and therefore, longer pulse durations will be used to allow enough heating of the dermal structures. In case the treatment is indicated for the treatment of post-acne scars, dermal coagulative necrosis combined with epidermal ablation is required, and therefore, medium pulse durations are used.⁸ It is important to test these different possible effects in a reliable and reproducible animal model. Here, we used the domestic pig, which is considered to be one of the best animal model for cutaneous evaluation.^{19,20} We utilized a complex and detailed experimental design enabling the evaluation of many energy levels and pulse durations over a large number of time points until complete healing is achieved. As expected, we observed power-related progressive performance from low to high power setting with a higher degree of coagulated tissue along the escalating power setting, peaking with ablations at the high-power setting. To the best of our knowledge, such detailed evaluation of fractional RF effects in domestic pigs has not been reported before, and the literature is restricted to studies using small animal numbers and evaluation of limited RF parameters.^{17,21}

While the use of fractional RF devices is usually considered safe, their use has been connected to complications, such as scarring, pigmentary changes, purpura, and erosions.²² Therefore, evaluation of the safety of new devices, and particularly the different parameters that are available in the specific device being tested, is essential and is considered a vital part of FDA regulations.²³ In accordance with the increasing number of medical devices being developed, information on preclinical animal trials with such devices is also growing.^{24–28} Specifically for fractional RF devices, it is important to evaluate the consistency and lack of fractional RF effects in the tissue adjacent to the application site, and the lack of any inflammatory reaction at the surrounding tissue. Furthermore, it is essential to observe that

normal wound healing process takes place in the application site, with formation of normal skin at this site.⁵ A single treatment with the fractional RF device in domestic pigs, in all evaluated parameters, including the worst-case scenarios, was not associated with local adverse effects apart from the desired induced necrosis, both macroscopically and microscopically and therefore is considered safe for use up to the tested high power setting. A trend for time-related progressive healing was noted both macroscopically and microscopically and reached complete healing by 7 days post application with minimally observed erythema at the higher power-treated sites. This erythema was not considered as adverse, was not associated with inflammatory reaction or pain, and is part of the normal reaction of the skin to the RF treatment.

The normal healing and the absence of adverse effects, such as burns or scar formation, further support the safety of the SVC technology, which is important for skin resurfacing treatments in humans. The power-related progressive increase in the incidence of ablation and coagulative necrosis from low to high power settings indicates that the efficacy of the device for different skin condition can be translated to the settings required for each skin condition. For example, high power settings with Shallow program lead to ablation of the epidermal layer, which produce a resurfacing effect, but coagulative necrosis of the deep dermis with lower settings and Deep program produces a skin rejuvenation effect that improves the appearance of post acne scars.⁸

We believe that the information provided here will be of value for future preclinical studies with new fractional or non-fractional RF devices and will provide details on the normal and expected tissue reaction to both ablative and coagulative necrosis effects of such devices.


Declaration of Conflicting Interests

The author(s) declared the following potential conflicts of interest with respect to the research, authorship, and/or publication of this article. Inna Belenkey is an employee of Viora Ltd.

Funding

The author(s) disclosed receipt of the following financial support for the research, authorship, and/or publication of this article: The study was funded by Viora Ltd, New York, NY, USA.

ORCID iD

Yuval Ramot  <https://orcid.org/0000-0002-8606-8385>

Supplemental Material

Supplemental material for this article is available online.

References

1. Husain Z, Alster TS. The role of lasers and intense pulsed light technology in dermatology. *Clin Cosmet Investig Dermatol*. 2016;9(3):29-40.
2. Seago M, Shumaker PR, Spring LK, et al. Laser treatment of traumatic scars and contractures: 2020 international consensus recommendations. *Lasers Surg Med*. 2020;52(2):96-116.

3. Alster TS, Tanzi EL, Lazarus M. The use of fractional laser photothermolysis for the treatment of atrophic scars. *Dermatol Surg.* 2007;33(3):295-299.
4. Kravvas G, Al-Niaimi F. A systematic review of treatments for acne scarring. Part 2: energy-based techniques. *Scars Burn Heal.* 2018;4:2059513118793420.
5. Hruza G, Taub AF, Collier SL, Mulholland SR. Skin rejuvenation and wrinkle reduction using a fractional radiofrequency system. *J Drugs Dermatol.* 2009;8(3):259-265.
6. Elsaie ML. Cutaneous remodeling and photorejuvenation using radiofrequency devices. *Indian J Dermatol.* 2009;54(3):201-205.
7. Kleidona IA, Karypidis D, Lowe N, Myers S, Ghanem A. Fractional radiofrequency in the treatment of skin aging: an evidence-based treatment protocol. *J Cosmet Laser Ther.* 2019:1-17.
8. Elman M, Gauthier N, Belenky I. New vision in fractional radiofrequency technology with switching, vacuum and cooling. *J Cosmet Laser Ther.* 2015;17(2):60-64.
9. Manstein D, Herron GS, Sink RK, Tanner H, Anderson RR. Fractional photothermolysis: a new concept for cutaneous remodeling using microscopic patterns of thermal injury. *Lasers Surg Med.* 2004;34(5):426-438.
10. Hantash BM, Mahmood MB. Fractional photothermolysis: a novel aesthetic laser surgery modality. *Dermatol Surg.* 2007;33(5):525-534.
11. Al-Niaimi F. Laser and energy-based devices' complications in dermatology. *J Cosmet Laser Ther.* 2016;18(1):25-30.
12. Brightman L, Goldman MP, Taub AF. Sublative rejuvenation: experience with a new fractional radiofrequency system for skin rejuvenation and repair. *J Drugs Dermatol.* 2009;8(11 Suppl):s9-s13.
13. Thanasarnakorn W, Siramangkhalanon V, Duncan DI, Belenky I. Fractional ablative and nonablative radiofrequency for skin resurfacing and rejuvenation of Thai patients. *J Cosmet Dermatol.* 2018;17(2):184-192.
14. Wang S, Manudhane A, Ezaldein HH, Scott JF. A review of the FDA's 510(k) approvals process for electromagnetic devices used in body contouring. *J Dermatolog Treat.* 2019;30(7):727-729.
15. Harth Y, Frank I. In vivo histological evaluation of non-insulated micro-needle radiofrequency applicator with novel fractionated pulse mode. *J Drugs Dermatol.* 2013;12(12):1430-1433.
16. Li X, Fang L, Huang L. In vivo histological evaluation of fractional ablative microplasma radio frequency technology using a roller tip: an animal study. *Lasers Med Sci.* 2015;30(9):2287-2294.
17. Shin MK, Choi JH, Ahn SB, Lee MH. Histologic comparison of microscopic treatment zones induced by fractional lasers and radiofrequency. *J Cosmet Laser Ther.* 2014;16(6):317-323.
18. Schafer KA, Eighmy J, Fikes JD, et al. Use of severity grades to characterize histopathologic changes. *Toxicol Pathol.* 2018;46(3):256-265.
19. Montagna W, Yun JS. The skin of the domestic pig. *J Invest Dermatol.* 1964;42(3):11-21.
20. Rittie L. Cellular mechanisms of skin repair in humans and other mammals. *J Cell Commun Signal.* 2016;10(2):103-120.
21. Sadick NS, Sato M, Palmisano D, Frank I, Cohen H, Harth Y. In vivo animal histology and clinical evaluation of multisource fractional radiofrequency skin resurfacing (FSR) applicator. *J Cosmet Laser Ther.* 2011;13(5):204-209.
22. Metelitsa AI, Alster TS. Fractionated laser skin resurfacing treatment complications: a review. *Dermatol Surg.* 2010;36(3):299-306.
23. Zuckerman DM, Brown P, Nissen SE. Medical device recalls and the FDA approval process. *Arch Intern Med.* 2011;171(11):1006-1011.
24. Ramot Y, Kannan K, Reddy S, Krishnappa H, Dillberger JE, Nyska A. Acute histopathologic findings related to needle puncture trauma during subcutaneous injection in the Sprague-Dawley rat model. *Toxicol Pathol.* 2019;47(1):93-96.
25. Ramot Y, Kronfeld N, Steiner M, et al. Biodegradability and safety study of LifeMesh, a novel self-adhesive mesh, in Sprague-Dawley rats. *Toxicol Pathol.* 2019;47(4):483-493.
26. Ramot Y, Rousselle SD, Yellin N, et al. biocompatibility and systemic safety of a novel implantable annuloplasty ring for the treatment of mitral regurgitation in a minipig model. *Toxicol Pathol.* 2016;44(5):655-662.
27. Ramot Y, Schiffenbauer YS, Amouyal N, et al. Compact MRI for the detection of teratoma development following intrathecal human embryonic stem cell injection in NOD-SCID mice. *Neurotoxicology.* 2017;59:27-32.
28. Rousselle SD, Ramot Y, Nyska A, Jackson ND. Pathology of bioabsorbable implants in preclinical studies. *Toxicol Pathol.* 2019;47(3):358-378.